

Magnetic Properties of Uniaxial Synthetic Antiferromagnetic  
Films

G. Mankey – University of Alabama  
et al.

Deposited 07/11/2019

Citation of published version:

Zhao, Z., et al. (2004): Magnetic Properties of Uniaxial Synthetic Antiferromagnetic  
Films. *Journal of Applied Physics*, 95(11). DOI: <https://doi.org/10.1063/1.1652417>

# Magnetic properties of uniaxial synthetic antiferromagnetic films

Cite as: Journal of Applied Physics **95**, 7157 (2004); <https://doi.org/10.1063/1.1652417>  
Published Online: 25 May 2004

Zhiya Zhao, Prakash Mani, W.-T. Lee, and Gary J. Mankey



View Online



Export Citation

## ARTICLES YOU MAY BE INTERESTED IN

[Strong anisotropy in thin magnetic films deposited on obliquely sputtered Ta underlayers](#)  
Journal of Applied Physics **88**, 5296 (2000); <https://doi.org/10.1063/1.1323436>

[Characterization of surface structure in sputtered Al films: Correlation to microstructure evolution](#)  
Journal of Applied Physics **85**, 876 (1999); <https://doi.org/10.1063/1.369206>

[Observation of rotatable stripe domain in permalloy films with oblique sputtering](#)  
Journal of Applied Physics **112**, 093907 (2012); <https://doi.org/10.1063/1.4764311>

A horizontal banner for Alluxa. On the left is the Alluxa logo, a stylized 'A' with a blue and orange gradient. To its right is the text 'Alluxa' in a large, white, sans-serif font. Further right is the text 'YOUR OPTICAL COATING PARTNER' in a smaller, white, sans-serif font. On the far right is a blue rectangular button with a white right-pointing arrow and the text 'DOWNLOAD THE LIDAR WHITEPAPER' in white, sans-serif font.

 Alluxa YOUR OPTICAL COATING PARTNER  DOWNLOAD THE LIDAR WHITEPAPER

# Magnetic properties of uniaxial synthetic antiferromagnetic films

Zhiya Zhao and Prakash Mani

*MINT Center, The University of Alabama, Tuscaloosa, Alabama 35487*

W.-T. Lee

*Spallation Neutron Source, Oak Ridge National Laboratory, Oak Ridge, Tennessee 37831*

Gary J. Mankey<sup>a)</sup>

*MINT Center, The University of Alabama, Tuscaloosa, Alabama 35487*

(Presented on 8 January 2003)

A study of the properties of uniaxial synthetic antiferromagnetic films with the structure Si(100)/Ta(5 nm)/Co(a)/NM(b)/Co(c)/Ta(10 nm) prepared by oblique sputtering is reported. Easy axis and hard axis hysteresis loops show a strong uniaxial anisotropy. The structural origin of the anisotropy is revealed by atomic force microscopy. The magnetization switching process was measured by polarized neutron reflectometry. The system exhibits biquadratic coupling, since the experimental remanence differs from that calculated by a model considering only bilinear coupling. The dependence of the critical fields on top ferromagnetic layer thickness is measured. A fit including both bilinear and biquadratic coupling qualitatively agrees with the results. © 2004 American Institute of Physics. [DOI: 10.1063/1.1652417]

## I. INTRODUCTION

Since the discovery of antiferromagnetic exchange coupling by Grünberg *et al.*,<sup>1</sup> synthetic antiferromagnet (SAF) structures have been studied extensively due to their application in recording media, read heads, and magnetic random access memory (MRAM) devices. The coupling between the magnetic layers is usually characterized by the coexistence of bilinear and biquadratic coupling mechanisms.<sup>2</sup> In addition, anisotropy is an important parameter for controlling magnetization in magnetic devices and determining the upper limit of susceptibility in magnetic thin films. For media applications, no in-plane anisotropy is needed, while in-plane anisotropy is preferred for head and MRAM applications where the magnetization switching occurs by coherent rotation.<sup>3</sup>

A strong in-plane uniaxial anisotropy can be generated in SAF structures by the anisotropic roughness of an obliquely sputtered Ta underlayer.<sup>4</sup> This article reports the magnetic properties of uniaxial synthetic antiferromagnetic (USA) structures which are SAF structures deposited on obliquely sputtered Ta layers.

## II. EXPERIMENT

USA structures were prepared in an ultraclean sputtering system as a function of bottom Co layer thickness,  $a$ , non-magnetic (NM) spacer layer thickness,  $b$ , and top Co layer thickness,  $c$ , on naturally oxidized Si (100) substrates with a background pressure of  $5 \times 10^{-9}$  mbar and working pressure of  $4.5 \times 10^{-5}$  mbar of ultrapure Ar. A 5 nm Ta underlayer was obliquely sputtered at  $60^\circ$  with respect to the surface normal to create a strong in-plane uniaxial anisotropy.<sup>4</sup> The subsequent layers of Co, Ru, and Ir were deposited at  $45^\circ$

incidence. All the samples have the configuration of Si(100)/Ta(5 nm)/Co(a)/NM(b)/Co(c)/Ta(10 nm), where NM is a nonmagnetic spacer layer, either Ir or Ru.

Magnetic properties were measured by an alternating gradient magnetometer, and the surface morphology of the obliquely sputtered Ta underlayer was measured using a Nanoscope IV Atomic Force Microscope (AFM). The polarized neutron reflectometer (PNR) POSY1 at the Intense Pulsed Neutron Source beamline c2 at Argonne National Lab was used to determine the magnetic reversal process of the USA structures.

## III. RESULTS AND DISCUSSION

The NM spacer material and thickness was first adjusted to the thickness where the magnetic coupling strength is nearly constant for small  $<0.05$  nm variations in NM thickness. For  $b=0.6$  nm and NM=Ru, both strong and stable interlayer exchange coupling was achieved. Figure 1(a) shows in-plane easy axis and hard axis hysteresis behavior of a typical USA structure. The hard axis lies in the Ta underlayer incidence plane while the easy axis lies perpendicular to the Ta incidence plane. A strong in-plane uniaxial anisotropy is evident from the hysteresis loops. Going from positive high field to low field, the easy axis loop shows a reorientation of the thin bottom Co layer from parallel to the external field to canted and finally to antiparallel with the external field and the thick Co layer magnetization. The easy axis loop shows sharp magnetization changes at  $H_{cr1}$  and  $H_{cr2}$  which separate the antiparallel, canted, and saturation states. When the field is swept in the negative direction from zero, an abrupt change in magnetization occurs when the magnetizations of both Co layers simultaneously change direction. The hard axis loop shows the magnetizations of the two Co layers first being aligned parallel to the external field at saturation, and gradually rotating to a canted magnetization configuration as the field is reduced. The gradual de-

<sup>a)</sup> Author to whom correspondence should be addressed; electronic mail: gmankey@mint.ua.edu

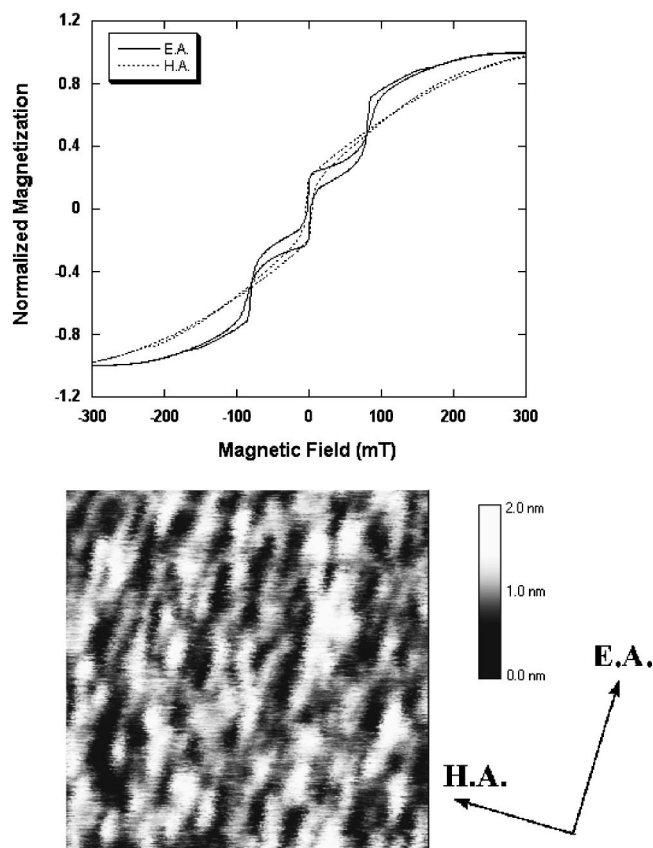


FIG. 1. (a) Normalized easy axis and hard axis hysteresis loops for Si(100)/Ta(5 nm)/Co(4.4 nm)/Ru(0.6 nm)/Co(8.8 nm)/Ta(10 nm) sample. (b) AFM image shows the topography of the obliquely sputtered 5 nm Ta underlayer. The scan was made on  $250 \times 250 \text{ nm}^2$  surface.

crease in the magnetization component parallel to the applied field occurs when the open angle between the two Co layer magnetizations increases.

In Fig. 1(b), the AFM image (250 nm square) of the as-deposited obliquely sputtered 5 nm Ta underlayer shows the structural origin of the anisotropy. One can observe that oblique deposition produces anisotropic roughness with ridges and grooves extending perpendicular to the Ta incidence direction. The presence of roughly aligned ridges and grooves is the origin of the magnetostatic anisotropy. The magnetic easy axis was later confirmed to be along the ridges and the hard axis perpendicular to the ridges.

To confirm the magnetic structure of the USA structures, we carried out PNR measurements.<sup>5-7</sup> The polarized neutron reflectivity of the sample with  $a = 13 \text{ nm}$ ,  $\text{NM} = \text{Ru}$  and  $b = 0.6 \text{ nm}$ , and  $c = 4.4 \text{ nm}$  was measured in a saturation field of 3 kOe and at a lower field of 200 Oe where the Co layers are believed to be antiferromagnetically aligned. The measurement temperature was 145 K. During the measurements, pulses of polarized neutrons with a wavelength  $\lambda$  from 2 to 14 Å impinged the sample at a grazing incident angle  $\theta < 1^\circ$ . The polarized neutron reflectivity as a function of the momentum transfer perpendicular to the sample surface,  $q_z = 4\pi \sin \theta / \lambda$ , were recorded and shown in Fig. 2.  $R^+$  and  $R^-$  correspond to the reflectivity of incident neutrons polarized parallel and antiparallel to the applied field, respectively.

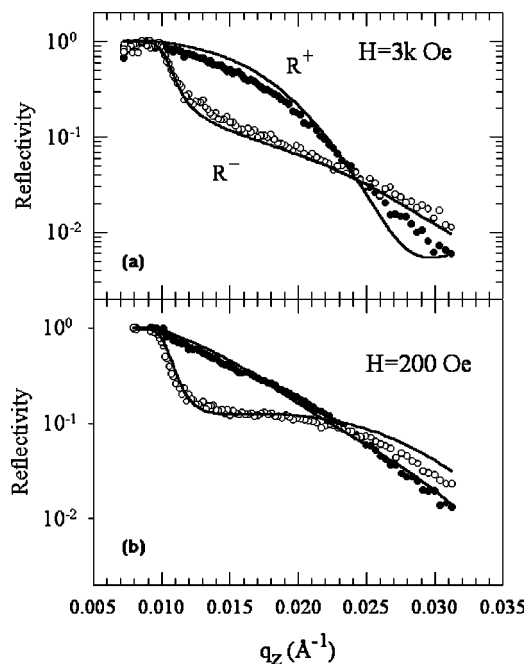


FIG. 2. Polarized neutron reflectivity as a function of the momentum transfer  $q_z$  (a) at saturation and (b) at 200 Oe where the Co layers coupled antiferromagnetically.  $R^+$  (closed symbol) and  $R^-$  (open symbol) were reflectivities measured with the incident parallel and antiparallel to the applied field, respectively. The solid curves show the result of curve fitting.

Polarized neutron reflectivity measures the Fourier components of the chemical and magnetic depth profile. The reflectivity can be fitted (solid curves in Fig. 2) to a model of the sample to obtain the thickness and magnetization of individual layers. The data in Fig. 2(a) is fitted assuming both Co layers have their magnetization vectors aligned with the field. The same sample was then measured in a reduced field of 200 Oe, Fig. 2(b). For these data, the curve fitting to the reflectivity measured at 200 Oe allowed only the magnetization of the Co layers to vary. The model that produces the best fit indicated that the Co layers are aligned antiparallel to each other, with the magnetic moment of the thinner Co layer opposite to the applied field and the thicker Co layer parallel to the applied field. Thus, the PNR measurements confirm that when the sample magnetization changes from saturation to antiferromagnetic state by reducing the applied field, the moments in the thinner Co layer rotate first. The results at negative saturation (not shown) confirmed the reversal of the moments in both Co layers as expected.

Ir and Ru were selected as spacer materials since Ru and Ir have the strongest coupling force as reported by Parkin.<sup>8</sup> Figure 3 shows a comparison between an easy axis saturation field  $H_{\text{sat}}$  of USA structures with different Ir and Ru spacer thicknesses in the range of the first peak of antiferromagnetic coupling. The USA structures have a configuration of Ta(5 nm)/Co(4.4 nm)/Ru(b)/Co(4.4 nm)/Ta(10 nm) and Ta(5 nm)/Co(4.4 nm)/Ir(b)/Co(4.4 nm)/Ta(10 nm). These results show that Ru has a stronger coupling force through a broader thickness range than Ir. The thickness range of Ru which shows a strong coupling force extends from 0.5 nm to 0.7 nm, so using a Ru layer allows for a larger tolerance in absolute thickness.

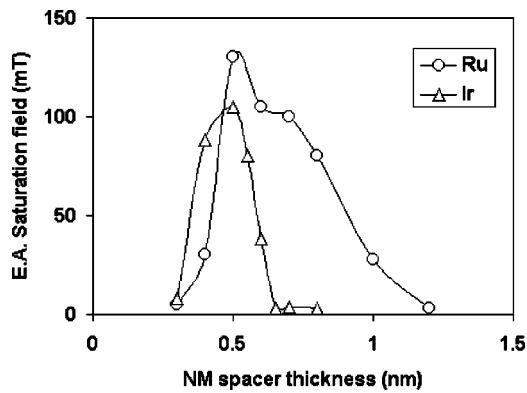


FIG. 3. Dependence of easy axis saturation field of NM spacer layer thickness.

Samples with Ta(5 nm)/Co(4.4 nm)/Ru(0.6 nm)/Co(*c*)/Ta(10 nm) were made in a perpendicular external field of 15 Oe (produced by the Ir magnetron gun), where the top layer Co thickness *c* is in the range of 8.8 to 44 nm. Figure 4(a) shows a comparison between the experimental remanence value and value calculated by the simple formula  $(c - a)/(c + a)$  which considers only bilinear coupling. The discrepancy between the experiment and the calculation value is due to the biquadratic coupling component. One can observe that the biquadratic coupling component decreases with the increase of the top Co layer thickness and becomes negligible when the top Co layer thickness increases to 35.2 nm.

In addition, we observed that the effective coupling constant also depends on the top ferromagnetic layer thickness,

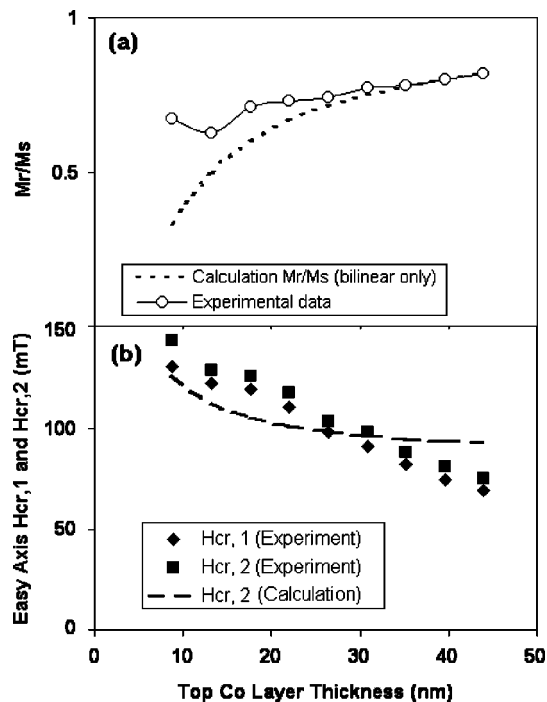


FIG. 4. (a) Comparison of experimental remanence with a calculation which only considers bilinear coupling. The difference is due to biquadratic coupling. (b) Dependence of easy axis critical fields  $H_{cr1}$  and  $H_{cr2}$  on top layer Co thickness.

*c*. Figure 4(b) shows the easy axis critical fields  $H_{cr1}$  and  $H_{cr2}$  as a function of the top layer Co thickness, *c*, for samples with  $a = 4.4$  nm and  $b = 0.6$  nm. The dotted line is a fit to<sup>9</sup>

$$H_{cr2} = \frac{1}{2M} \left( \frac{1}{a} - \frac{1}{c} \right) (j_1 + j_2) + \frac{1}{M} \times \sqrt{\left[ \frac{1}{2} \left( \frac{1}{a} - \frac{1}{c} \right) (j_1 + j_2) + 2K_u \right]^2 + \frac{4K_u(j_1 + j_2)}{c}}, \quad (1)$$

where *M* is the saturation magnetization for Co,  $K_u$  is induced uniaxial anisotropy,  $j_1$  and  $j_2$  are, respectively, the bilinear and biquadratic exchange coupling constants. This equation was obtained by an energy minimization calculation of a phenomenological expression for areal energy density in a SAF structure.<sup>9</sup> A coherent rotation mechanism was assumed in the magnetic reversal process for the SAF structure. The fit qualitatively agrees with experiment result. The effective coupling strength decreases with the top Co layer thickness.

#### IV. CONCLUSION

The USA structures have been produced by oblique sputtering. Strong antiferromagnetic coupling was observed in the sample with 0.6 nm Ru spacer layer. Distinguishable easy axis and hard axis hysteresis loops show existence of strong uniaxial anisotropy in the USA structures. PNR directly reveals the switching process of the USA structure when the magnetic field swept from positive to negative. There is a significant difference between the experimental remanence and the value calculated by the model which considers only bilinear coupling. This indicates there is a coexistence of bilinear and biquadratic coupling in the USA structure. A dependence on top ferromagnetic layer thickness of the critical fields  $H_{cr1,2}$  were observed. A fit including both bilinear and biquadratic coupling factors qualitatively agrees with experiment result. This further verifies the coexistence of bilinear and biquadratic mechanism.

#### ACKNOWLEDGMENTS

This project was supported by the National Science Foundation through the Materials Research Science and Engineering Center Grant No. DMR-0213985 at the University of Alabama. The authors want to express their gratitude to Dr. Suzanne te Velthuis for her assistance in the PNR experiment.

<sup>1</sup>P. Grunberg, R. Schreiber, Y. Pang, M. B. Brodsky, and H. Sowers, Phys. Rev. Lett. **57**, 2442 (1986).  
<sup>2</sup>S. O. Demokritov, J. Phys. D **31**, 925 (1998).  
<sup>3</sup>T. G. S. M. Rijks, W. J. M. de Jonge, W. Folkerts, J. C. S. Kools, and R. Coehoorn, Appl. Phys. Lett. **65**, 916 (1994).  
<sup>4</sup>R. D. McMichael, C. G. Lee, J. E. Bonevich, P. J. Chen, W. Miller, and W. F. Egelhoff, Jr., J. Appl. Phys. **88**, 5296 (2000).  
<sup>5</sup>J. F. Ankner and G. P. Felcher, J. Magn. Magn. Mater. **200**, 741 (1999).  
<sup>6</sup>C. F. Majkrzak, Physica B **221**, 342 (1996).  
<sup>7</sup>H. Zabel, R. Siebrecht, and A. Schreyer, Physica B **276**, 17 (2000).  
<sup>8</sup>S. S. P. Parkin, Phys. Rev. Lett. **67**, 3598 (1991).  
<sup>9</sup>K. Zhang, T. Kai, T. Zhao, H. Fujiwara, and G. J. Mankey, J. Appl. Phys. **89**, 6814 (2001).